Sound localization at high frequencies and across the frequency range

Petr Marsalek[a,c,d]**, Jiri Kofranek**[b,c]

[a] Tel.: ++(420) 224 965 901; Fax: ++(420) 224 912 834;

E-mail: marsalek@karlin.mff.cuni.cz

[b] Tel.: ++(420) 224 965 901; Fax: ++(420) 224 912 834;

E-mail: kofranek@cesnet.cz

[c] *Charles University Prague, Department of pathological physiology,*

U nemocnice 5, Praha 2, CZ-128 53, Czech Republic

[d] corresponding author

Abstract

Mammal sound localization uses two distinct neural circuits, one for low and one for high frequency. We explain why the coincidence detection at the neuronal level is used in both pathways. Our description is based on probabilistic spiking and timing jitter. We propose a new inhibitory coincidence detection mechanism for the inhibitory part in the high frequency pathway. Output firing and gain of the two mechanisms is calculated. We show how the output gains of the mechanisms predict the notch within the frequency sensitivity range. This notch was described in human psychophysical experiments.

Keywords: Sound localization pathway, Time jitter, Coincidence detection, Medial and lateral superior olive

1 Introduction

The direction of sound is computed in two branches of the auditory pathway. The first branch has an important relay station in the medial superior olive (MSO) and process lower frequencies. Higher frequencies are processed in the lateral superior olive (LSO). Both the MSO and the LSO are the first nuclei in the sound localization pathway, which collect inputs from both sides. To achieve sufficient time precision, in both systems, coincidence detection (CD) is the spike generation mechanism. In an old result by Srinivasan and Bernard, [17], CD is shown to give a multiplication of firing rates. They assume asynchronous spike trains as input. We have adapted their observations for synchronous spike trains. We propose two variants of spike generation mechanisms, which are consistent with real spike trains statistics. To distinguish them, we call them excitatory coincidence detection (ECD) and inhibitory coincidence detection (ICD). As in [17], the mechanisms include timing **jitter** (random delay in spike arrival, denoted Δ_J) and **probabilistic spike delivery** (denoted p_D). Experimentally observed synchronization precision in MSO and LSO is the highest spike timing precision ever described in neural systems. We study how does the system cope with the jittery spike propagation.

In the MSO the sound direction clue is the disparity of timing (ie. phase) between the two ears, interaural time delay. A classical theory of Jeffres [5] postulates that the right timing is picked up along the delay line, where individual neurons are specialized as CDs. The classical theory for the LSO states that the disparity of sound level between the two ears, interaural level difference, is calculated via subtraction of firing rates (SFR) of two inputs. From the excitatory input at ipsilateral side is subtracted the inhibitory input at contralateral side [6].

We have shown previously that neurons perform coincidence detection thanks to the specific dynamics of ion channels [10]. Our simulation and theory, and also similar theory by other authors [1], were based on experiments in chicken brainstem slices [15, 16]. We also studied limits, which are imposed upon the CD mechanism basically by a presence of refractory period and firing stochasticity [11]. The ECD described here takes place in MSO (this agrees with previous theories,

we only show the spike statistics differently) and further we describe the ICD. We assume that the ICD is implemented in LSO (this is a novel theory, described here and in [12] for the first time).

2 Description of the mechanisms and results

2.1 Coincidence detection mechanisms

We will describe spike generation mechanisms as calculation with spikes. For biological context we refer to the Discussion section. Spike trains in both sides derive from the sound input. For the purpose of following calculations, all neural events will be written as functions of time. Let us write the sound input as a periodic train $S_{\mathrm{Z}} = \sum_{i=1}^{n} \delta(t - iT_{\mathrm{Z}})$, of the Dirac delta pulses δ, where $T_{\mathrm{Z}} = f_{\mathrm{Z}}^{-1}$ is the period of the sound (inverse of its frequency). Train of spikes at times $T_1, T_2, ..., T_n$ will be written as $\sum_{i=1}^{n} \delta(t - T_i)$. We can also write spike trains at sides A and B as $\sum_{i=1}^{n} X_{\mathrm{A}i}\delta(t - J_{\mathrm{A}i} - iT_{\mathrm{Z}})$ and $\sum_{i=1}^{n} X_{\mathrm{B}i}\delta(t - J_{\mathrm{B}i} - iT_{\mathrm{Z}})$, where $J_{\mathrm{A}i}$ and $J_{\mathrm{B}i}$ (spike timing **jitter** instances) are a series of independent random variables drawn from the uniform probability density function with height Δ_J^{-1}, (with the mean $E(J) = 0$ and standard deviation $Std(J) = \frac{\sqrt{3}}{6}\Delta_{\mathrm{J}}$. This probability density function has been used for jitter before [2].) It is nonzero only within the span of the timing jitter and also it is the simplest to calculate. $X_{\mathrm{A}i}$ and $X_{\mathrm{B}i}$ are series of discrete random variables attaining 1 with probabilities of p_{DA} and p_{DB}, and 0 with probabilities of $1 - p_{\mathrm{DA}}$ and $1 - p_{\mathrm{DB}}$, respectively (these are the **probabilities of spike delivery**). Denote with ρ a rectangular pulse of height 1 starting at the time 0 and with the duration Δ as $\rho(1, \Delta)(t)$. Using this ρ, series of windows of duration Δ_{CD} following spike train can be written as $W = \sum_{i=1}^{n} \rho(1, \Delta_{\mathrm{CD}})(t - T_i)$.

2.2 Excitatory coincidence detection

In excitatory CD, spike is generated when the spikes from both trains are closer in time than Δ_{CD}: $(t - J_{\mathrm{A}i} - iT_{\mathrm{Z}}) - (t - J_{\mathrm{B}i} - iT_{\mathrm{Z}}) = J_{\mathrm{A}i} - J_{\mathrm{B}i} < \Delta_{\mathrm{CD}}$. Following [17], let W_{A} and W_{B} be series of windows (spikes filtered by the CD mechanism) with the duration Δ_{CD}. If these windows overlap, coincidence is detected. The mechanism of summing the windows is shown in the left panel of

Figure 1. The train of output windows is:

$$W_{AB} = W_A + W_B = \sum_{i=1}^{n} X_{Ai}\rho(1,\Delta_{CD})(t - J_{Ai} - iT_Z) + X_{Bi}\rho(1,\Delta_{CD})(t - J_{Bi} - iT_Z) \quad (1)$$

Insert *Fig. 1* **around here**

Assume further that $\Delta_{CD} < \Delta_J$. Then in one cycle the window W_{AB} should attain the value of 2 with the probability $p_{DA}p_{DB}P(J_A - J_B < \Delta_{CD})$. We will now ask, what is the probability p_{CD} that the two pulses will meet within the time window Δ_{CD}? For independent J_A and J_B, the random variable $J_2 = J_A - J_B$ has a probability density function $-\Delta_J^{-2}t + \Delta_J^{-1}$ for $t \geq 0$ and $\Delta_J^{-2}t + \Delta_J^{-1}$ for $t \leq 0$. Then the probability p_{CD} is:

$$p_{CD} = P(J_A - J_B < \Delta_{CD}) = P(J_2 < \Delta_{CD}) = 2\int_0^{\Delta_{CD}} \Delta_J^{-2}t + \Delta_J^{-1}dt = \Delta_{CD}(2\Delta_J - \Delta_{CD})/\Delta_J^2, \quad (2)$$

We will now use the probability p_{CD} to estimate the firing frequency f_{ECD} of the ECD mechanism. It will be fraction of input sound frequency multiplied by probabilities of independent events:

$$f_{ECD} \leq f_Z p_{DA} p_{DB} \Delta_{CD}(2\Delta_J - \Delta_{CD})/\Delta_J^2. \quad (3)$$

The right side overestimates f_{ECD}, therefore we write the inequality here. It now remains to show, what are the probabilities of p_{DA} and p_{DB} depending on the value of f_Z. We assume that below certain sound frequency limit f_L all spikes propagate and $p_{DA} = p_{DB} = 1$ while above the limit frequency, $p_{DA} = p_{DB} = f_L/f_Z$ [11]. The product of functions dependent on f_Z can be written conveniently as $\psi(f_Z) = f_Z p_{DA} p_{DB}$. (With the use of the Heaviside step function, $H(x) = 0$ for $x < 0$ and $H(x) = 1$ for $x \leq 0$, we can write $\psi(f_Z) = f_Z H(f_L - f_Z) + f_Z^{-1}H(f_Z - f_L)$.) Limit frequencies of ECD and ICD for human listeners are $f_L = 750$ Hz for ECD and $f_L = 3$ kHz for ICD. f_{ECD} and f_{ICD} are shown in fig. 3.

Insert *Fig. 2* **around here**

The above mentioned calculation holds when the time jitter is set not to exceed the sound period: $\sqrt{2}\Delta_J < T_Z$, because $Std(J_2) = \sqrt{2}\Delta_J$. This way the time jitter will not cause the overlap of a spike over one sound cycle. Towards higher frequencies, when T_Z decreases and Δ_J stays fixed, this condition may not be fulfilled.

The requirement that must be $W_A = 1$ and $W_B = 1$ at the same time will be obtained using a threshold of the sum of the windows:

$$W_{\mathrm{A}} + W_{\mathrm{B}} > 1.5. \tag{4}$$

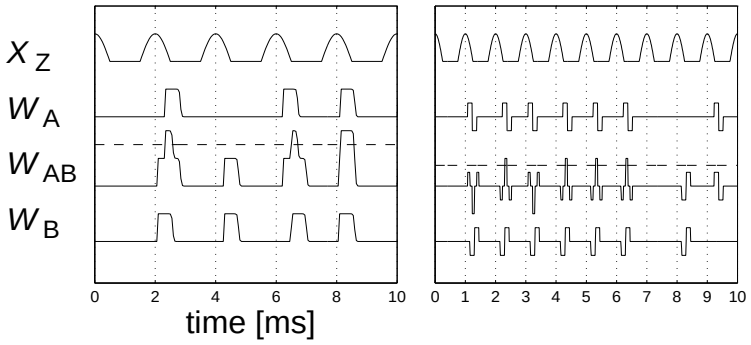

Figure 1: **Excitatory and inhibitory coincidence detection**

Left panel: excitatory CD and **right panel:** inhibitory CD. $X_{\mathrm{Z}} = \sum_{i=1}^{n} \rho(1,\pi)(2\pi f_{\mathrm{Z}} t + \pi/2 - iT_{\mathrm{Z}})\cos(2\pi f_{\mathrm{Z}} t)$ are half-waves of sound stimulus, the top trace. Traces W_{A} and W_{B} are traces of CD time windows of both sides and the middle trace W_{AB} is the output trace. The sample sound frequency in the left panel is $f_Z = 500$ Hz and in the right panel is $f_Z = 1$ kHz. Sizes and randomness of $J_{\mathrm{A}i}$, $J_{\mathrm{B}i}$ and Δ_{CD} are exaggerated for the sake of demonstration. Broken line shows the value of threshold, in both panels equal to 1.5.

2.3 Inhibitory coincidence detection

The train A, and also B, is again, as for ECD: $\sum_{i=1}^{n} X_{\mathrm{A}i}\delta(t - J_{\mathrm{A}i} - iT_{\mathrm{Z}})$. We will again use equation (1), this time we substitute into it windows consisting of two pulses, $\rho_2 = \rho(1,\Delta_{\mathrm{CD}})(t) - \rho(1,\Delta_{\mathrm{CD}})(t - \Delta_{\mathrm{CD}})$. If the window ρ_{B} comes before ρ_{A} by the time Δ_{AB}, then $\rho_{\mathrm{AB}} = \rho_{\mathrm{A}} + \rho_{\mathrm{B}} = -\rho(1,\Delta_{\mathrm{AB}})(t) + 2\rho(1,\Delta_{\mathrm{AB}})(t - \Delta_{\mathrm{CD}}) - \rho(1,\Delta_{\mathrm{AB}})(t - \Delta_{\mathrm{CD}})$. If ρ_{B} comes later, the sign of the previous expression is reversed, $\rho'_{\mathrm{AB}} = -\rho_{\mathrm{AB}}$. This is shown for ICD in the right panel of Figure 1. Clearly, the threshold in inequality (4) is exceeded only in the first case and not in the second. For the time Δ_{AB} set $\Delta_{\mathrm{AB}i} = \max(0, \Delta_{\mathrm{CD}} - J_{\mathrm{A}i} + J_{\mathrm{B}i})$. The condition in inequality (4) is fulfilled when

$J_A - J_B < \Delta_{CD}$. From this we further proceed as in equation (2): $P(J_A - J_B < \Delta_{CD}) = P(J_2 < \Delta_{CD})$

$$\int_0^{\Delta_{CD}} \Delta_J^{-2} t + \Delta_J^{-1} dt = \Delta_{CD}(2\Delta_J - \Delta_{CD})/\Delta_J^2, \quad (5)$$

And thus:

$$f_{ICD} \leq f_Z p_{DA} p_{DB} \Delta_{CD}(2\Delta_J - \Delta_{CD})/2\Delta_J^2 = \psi(f_Z)\Delta_{CD}(2\Delta_J - \Delta_{CD})/2\Delta_J^2. \quad (6)$$

which is up to the multiplicative constant $\frac{1}{2}$ identical to the expression (3) for f_{ECD}. The height of the threshold is the same as in (4), 1.5.

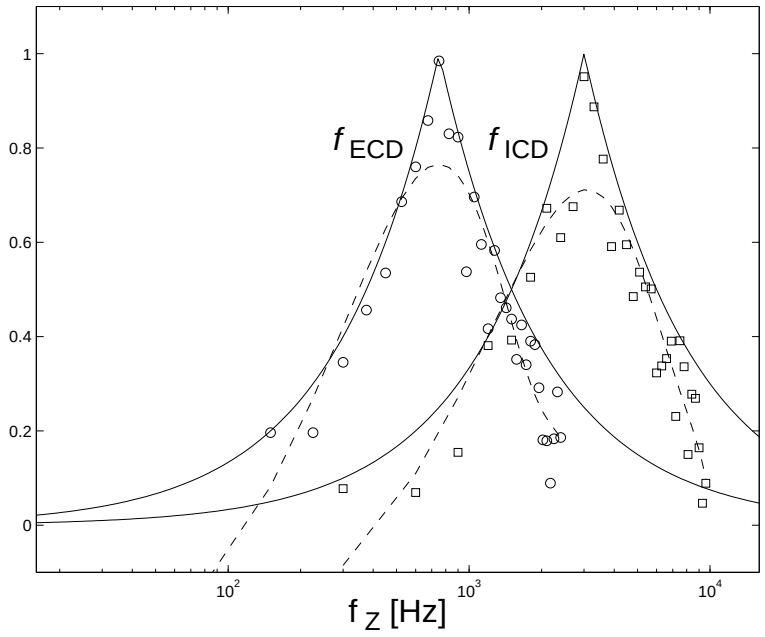

Figure 2: **Performance limits for excitatory and inhibitory coincidence detection**

x-axis: sound frequency f_Z in logarithmic scale, y-axis: gain in arbitrary units. Solid curves f_{ECD} and f_{ICD} show the absolute limits for CDs, they show where equality in the inequalities (3) and (6) holds. The gain of all instances of neurons will be lower or the same like the curve. The maximum gains (for a given neuron across the frequency range) are shown in circles for ECD in MSO and in squares for ICD in LSO. The two smoothed broken curves are obtained by the fitting of the 4th order polynomials to the data in circles and squares, respectively.

Insert *Fig. 3* **around here**

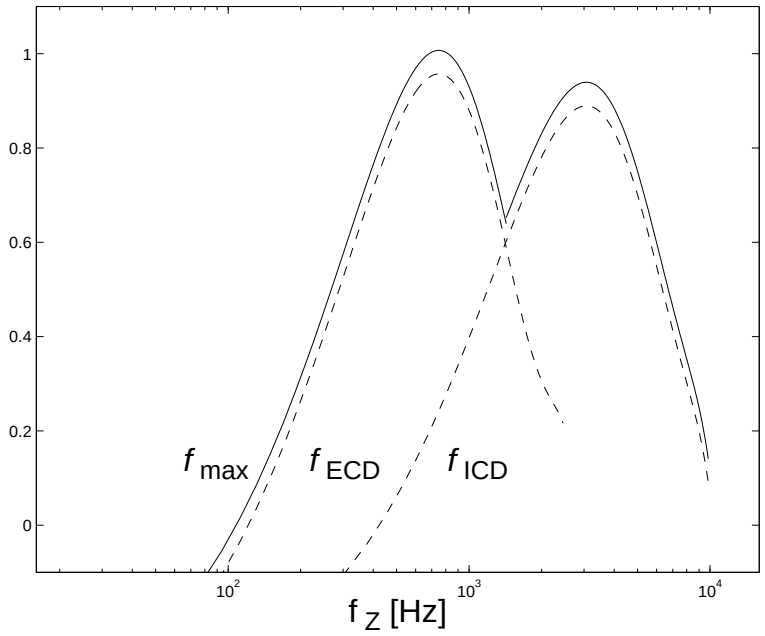

Figure 3: **Sensitivity notch between low and high frequencies**

x- and y-axes same as in figure 2. This is a prediction of what should be the best sound localization performance across the frequency range. This is obtained as maximum of two gains of the two CD mechanisms studied so far. The positions of the two peaks (f_L for ECD and for ICD, respectively) are chosen in order to reproduce the 1.5 kHz notch observed in human listeners [14]. The solid line of the predicted psychophysical curve is artificially shifted up by the value of 0.05 to be distinguishable from the broken lines.

2.4 Gains across the frequency range

Now the mechanisms introduced so far will be applied in the description of sound localization across the frequency range. The equality sign in inequalities (3) and (6) holds under assumption that neurons do not have preferential frequency and that spike occurence has the same probability at every sound cycle. Neurons tuned to a particular frequency spike at sub-harmonic frequencies of this frequency. Also the refractory period lowers the spiking probability at the first sound cycle after a spike. Thus the two above mentioned assumptions will lead to a lower firing rate than calculated by the equality sign in the two inequalities. Circles and squares in Figure 2 show several individual

neurons. All the data points are below or at the solid lines for equations in inequalities (3) and (6). Figure 3 shows the predicted perceptual performance of the system resulting as maximum performance of the two mechanisms. The gain curve contains the 1.5 kHz notch observed in human listeners [14].

3 Discussion

What is the neural site of the two CD mechanisms? We attribute the windows W following spikes to the low pass filtering nature of axons, synapses and dendrites. The window in the ICD with negative phase preceding the positive phase is just regular spike followed by the hyperpolarizing currents, but inverted, because it is passed through the inhibitory synapse. The ICD is an alternative mechanism to the SFR in the LSO. The SFR is postulated to take place in the LSO according to current opinion. The ICD has one advantage compared to the SFR: it is instantaneous, the resulting spike is generated within one sound cycle. In [12] we show, that in agreement with behavior the ICD is faster than the SFR. The probabilistic spike delivery and timing jitter are common concepts [2, 3, 7, 17].

The proposal of the ECD and the ICD mechanism is motivated by experiments [8]. The pioneer experiments of Goldberg and Brown [4] supported the Jeffres theory [5]. Some novel observations state that time differences and intensity differences are multiplexed along the two pathways and that the multiplexed signals are used in the population coding at the higher relays of the pathways, [13, 6]. This is also supported by the morphology of the high frequency pathway: it has large axons and synapses, which are the biggest in the mammalian CNS, [6]. We present a constructive critique of classical theories by suggesting a mechanism which: uses a precision observed in both the MSO and especially the LSO [6] and works with certain probability for every sound cycle. This can be compared to the leaky integrator with periodic input, studied in [9]. Kempter studied in [7] the properties of CD and give the explanation, why the threshold mechanism together with just a few excitatory postsynaptic potentials are most effective with biologically plausible synaptic dynamics.

Acknowledgment

Supported by Physiome.cz, Ministry of Education no. 111100008, Charles University no. 201352. Thanks to N. Dorrell.

References

[1] H. Agmon-Snir, C. E. Carr, and J. Rinzel. The role of dendrites in auditory coincidence detection. *Nature*, 393:268–272, 1998.

[2] J. F. Feng. Behaviors of spike output jitter in the integrate-and-fire model. *Physical Review Letters*, 79:4505–4508, 1997.

[3] W. Gerstner, R. Kempter, J. L. van Hemmen, and H. Wagner. A neuronal learning rule for sub-millisecond temporal coding. *Nature*, 383:76–78, 1996.

[4] J. M. Goldberg and P. B. Brown. Response of binaural neurons of dog superior olivary complex to dichotic tonal stimuli: Some physiological mechanisms of sound localization. *J. Neurophysiol.*, 32:613–636, 1969.

[5] L. A. Jeffress. A place theory of sound localization. *J. Comp. Physiol. Psychol.*, 41:35–39, 1948.

[6] P. X. Joris and T. C. Yin. Envelope coding in the lateral superior olive. I. Sensitivity to interaural time differences; II. Characteristic delays and comparison with the responses in the medial superior olive; III. Comparison with afferent pathways. *J. Neurophysiol.* I: 73(3):1043-1062, 1995; II: 76(4):2137-56, 1996; III: 79(1):253-69, 1998. I.-III. 1995-1998.

[7] R. Kempter, W. Gerstner, and J. L. van Hemmen. How the threshold of a neuron determines its capacity for coincidence detection. *Biosystems*, 48:105–112, 1998.

[8] M. Konishi. Similar algorithms in different sensory systems and animals. In *Cold Spring Harbor Symposia on Quantitative Biology*, pages 575–583. CSH Laboratory, New York, 1990.

[9] P. Lánský. Sources of periodical force in noisy integrate-and-fire models of neuronal dynamics. *Physical Review E*, 55(2):2040–2043, 1997.

[10] P. Marsalek. Coincidence detection in the Hodgkin-Huxley equations. *Biosystems*, 58(1-3):83–91, 2000.

[11] P. Marsalek. Neural code for sound localization at low frequencies. *Neurocomputing*, 38-40(1-4):1443–1452, 2001.

[12] P. Marsalek and J. Kofranek. Spike encoding mechanisms in sound localization pathway. *Submitted to Biosystems*, 2003.

[13] D. McAlpine, D. Jiang, and A. R. Palmer. A neural code for low-frequency sound localization in mammals. *Nat. Neuroscience*, 4(4):396–401, 2001.

[14] A. W. Mills. *Foundations of Modern Auditory Theory*, chapter Auditory Localization, pages 303–348. Academic Press, New York, 1972.

[15] A. D. Reyes, E. W. Rubel, and W. J. Spain. Membrane-properties underlying the firing of neurons in the avian cochlear nucleus. *J. Neuroscience*, 14:5352–5364, 1994.

[16] A. D. Reyes, E. W. Rubel, and W. J. Spain. *In-vitro* analysis of optimal stimuli for phase-locking and time-delayed modulation of firing in avian nucleus laminaris neurons. *J. Neuroscience*, 16:993–1007, 1996.

[17] M. V. Srinivasan and G. D. Bernard. A proposed mechanism for multiplication of neural signals. *Biol. Cybernetics*, 21:227–236, 1976.

Biosketches

Petr Marsalek received his MD in 1990, his BS in Computer Science in 1992 and his PhD in Biophysics in 1999, all degrees from the Charles University, Prague, The Czech Republic. Since 1993 he has been with the Department of Pathological Physiology, First Medical Faculty, Charles University. In the past, he spent several years as a postdoctoral fellow. He worked at the Caltech in the CNS Program and at the Johns Hopkins University in the Mind Brain Institute. He has currently submitted his ”habilitation” thesis at Charles University, to become an Associate Professor.

Jiri Kofranek received his MD in General Medicine in 1974 and his PhD in Normal and Pathological Physiology in 1982, both from Charles University, Prague. Since 1975 he has been with the Department of Pathological Physiology, First Medical Faculty, Charles University, now as an Assistant Professor. His main interests are in modeling homeostasis and the development of simulation and educational software. He has been the principal investigator of numerous grants in his field. In recent years he became a coordinator of the research initiative “physiome.cz”. He is currently the Head of the Biocybernetics Laboratory.